Journal of Chemical Crystallography
https://doi.org/10.1007/s10870-024-01023-4

ORIGINAL PAPER

Synthesis, Crystal Structure, and Properties of a Zn(II) Coordination Polymer from a New Semirigid Tripodal Nitrogen-Containing Heterotopic Ligand

Bing-Xun Zhou[1] · Xian Lin[1] · Hui-Qi Xie[1] · Liang-Hua Wu[1] · Chu-Hong Zhang[1] · Hai-Yan Song[1] · Jun Fan[1,2] · Sheng-Run Zheng[1]

Received: 13 March 2024 / Accepted: 11 July 2024

Abstract

A new coordination polymer, namely, $\{[Zn(DTPP)(H_2O)_2]\cdot H_2O\}_n$ (H_2DTPP = 3-(3,5-di(2H-tetrazol-5-yl)phenoxy)pyridine, compound **1**), was successfully assembled by using a new semirigid tripodal nitrogen-containing heterotopic ligand and characterized by single-crystal X-ray diffraction, elemental analysis, infrared spectroscopy, TG, and luminescence. X-ray single-crystal diffraction analysis revealed that compound 1 crystallizes in an orthorhombic crystal system with space groups of Ibca. It is a 2D coordination network with ($4{\cdot}8^2$) topology, and the 2D networks are further connected by hydrogen bonds between coordinated water molecules and tetrazole N atoms to form a 3D supramolecular framework. Moreover, compound **1** exhibits intense blue emission centered at 345 nm upon excitation at 276 nm and has the ability to sense Fe^{3+} via photoluminescence quenching.

Graphical Abstract

A new coordination polymer synthesized from a new semirigid tripodal nitrogen-containing heterotopic ligand, $\{[Zn(DTPP)(H_2O)_2]\cdot H_2O\}_n$, was characterized.

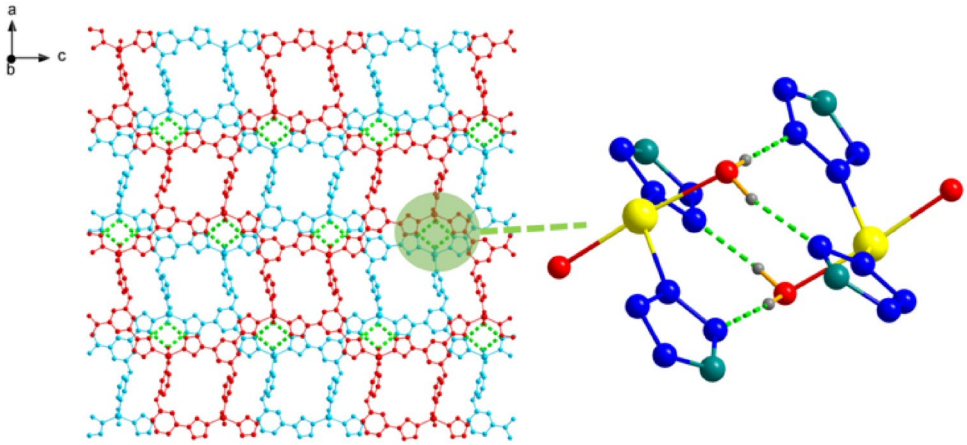

Keywords Coordination polymer · Tripodal heterotopic ligand · Crystal structure · Luminescence

Introduction

As new crystalline materials have diverse structures and extensive applications in gas adsorption and separation, catalysis, luminescent sensing, and so on [1–6], the

Extended author information available on the last page of the article

Published online: 22 July 2024

construction of coordination polymers (CPs) has still attracted much attention. In general, new CPs can be obtained by regulating their building blocks (such as organic ligands, metal ions, and counter anions) or/and assembly conditions (such as temperature, pH, concentration, and solvent). Among them, organic ligands play a main role in the formation of new CPs with desirable structures and properties. Tripodal nitrogen-containing ligands are a group of excellent ligands that have been applied to construct various coordination supramolecules, including CPs and metal-organic cages [7–12]. However, the most frequently used tripodal nitrogen-containing ligands are homotopic, and the three coordinating groups are identical. However, those based on heterotopic tripodal nitrogen-containing ligands have been relatively less explored [13].

Recently, we focused on the construction of new CPs based on a series of rigid tripodal nitrogen-containing ligands containing two kinds of donor groups, such as tetrazole-imdazole [13–17], tetrazole-pyridine [18, 19], and pyrazole-imidazole ligands [20, 21]. In this study, a new tetrazole-pyridine ligand, 3-(3,5-di(2H-tetrazol-5-yl) phenoxy)pyridine (H_2DTPP), was selected to construct new CPs. A Zn(II) CP with a 2D network structure was successfully obtained and well characterized by single-crystal X-ray diffraction, elemental analysis, and infrared spectroscopy. Additionally, the thermal stability and photoluminescence properties of the selected compounds were investigated in detail.

Experimental

Materials and Methods

The ligand H_2DTPP was purchased from Shanghai Kylpharm Co., Ltd., through its customized service. All the other reagents were of analytical grade quality and were obtained from Guangzhou Chemical Reagent Factory without further purification. Infrared (IR) spectroscopy was performed on a Nicolet FT-IR-170SX spectrometer with KBr pellets in the 400−4000 cm^{-1} region. Powder X-ray diffraction (PXRD) patterns were obtained by an Ultima IV diffractometer with a scan speed of 12°/min at 40 kV and 40 mA with a Cu-target tube and a graphite monochromator. Elemental analysis (C, H, and N) was performed with a Perkin-Elmer 240 C elemental analyzer. Thermogravimetric analysis (TGA) was performed on a NETZSCH STA 449 C thermogravimetric analyzer at a heating rate of 10 °C/min under a nitrogen atmosphere. The luminescent spectra for H_2DTPP and compound 1 were determined by using an Edinburgh FLS-900 spectrophotometer with a 150 W xenon lamp as the light source at room temperature.

Synthesis of Compound 1, $\{[Zn(DTPP)(H_2O)_2]\cdot H_2O\}_n$

A mixture of H_2DTPP (0.03 mmol, 9.2 mg), $Zn(NO_3)_2\cdot 6H_2O$ (0.06 mmol, 17.8 mg), methanol (1.5 mL), DMF (1.5 mL), and H_2O (3 mL) was stirred for 5 min. Then, the solution was sealed in a conical flask and left for 8 days to obtain pale yellow crystals in solution. The crystals were filtered and washed with deionized water and dried in air (yield: 53% based on H_2DTPP). Anal. Calcd. for $C_{104}H_{104}N_{72}O_{32}Zn_8$: C, 36.77; H, 3.09%; N, 29.68%; Found: C, 36.69%; H, 3.12%; N, 29.76%. IR (KBr pellet, cm^{-1}): 3222(*s*), 1620(*m*), 1574(*m*), 1438(*s*), 1243(*s*), 1120(*w*), 1060(*w*), 934(*m*), 887(*m*), 790(*m*), 691(*m*).

X–ray Crystallography

Single-crystal X-ray diffraction data for compound **1** were recorded on a Rigaku SuperNova Dual Atlas diffractometer with graphite-monochromated Cu Ka radiation (λ = 1.54184 Å) at 100 K. Data reduction, scaling, and absorption corrections were performed using CrysAlis^{Pro} 1.171.41.119a [22]. Empirical absorption correction using spherical harmonics was implemented in the SCALE3 ABSPACK scaling algorithm. Using Olex2 [23], structural solution and refinement based on F^2 were performed with the SHELXS-2018 and SHELXL-2018 program packages [24, 25], respectively. Anisotropic atomic displacement parameters were applied to all non-hydrogen atoms during refinement. The hydrogen atoms were added geometrically. The details of the crystal parameters, data collection, and refinement for the title compound are shown in Table 1, and selected bond lengths and angles are displayed in Table 2.

Results and Discussion

Description of the Crystal Structure

Single-crystal X-ray diffraction revealed that compound **1** crystallizes in an orthorhombic system with the space group *Ibca*. The asymmetric unit contains one Zn(II) ion, one $DTPP^{2-}$ ligand, two coordinated water molecules, and one uncoordinated water molecule. The Zn(II) ion adopts a five-coordinate triangular bipyramidal coordination mode, coordinating with two N atoms from two different tetrazole groups and one N atom from the pyridine group on the triangular plane and coordinating with two coordinated water molecules in the axial direction (Fig. 1). The Zn–N bond lengths range from 2.008(3) to 2.041(3) Å, and the Zn–O bond distances are 2.153(3) and 2.161(3) Å (Table 2), all of which are comparable to those observed for other related

Table 1 Crystallographic data and structure refinement for the title compound.

CCDC deposit No.	CCDC-2339096
Empirical formula	$C_{13}H_{13}N_9O_4Zn$
Formula weight	424.69
Temperature/K	100.00 10)
Wavelength/Å	11.54184
Crystal system	orthorhombic
Space group	*I*bca
a/Å	23.4842(4)
b/Å	12.9423(3)
c/Å	24.1939(5)
α/(°)	90
β/(°)	90
γ/(°)	90
V/Å^3	7353.5(3)
Z	16
D_c/(mg m^{-3})	1.534
μ/mm^{-1}	2.228
F (000)	3456
θ Range for data collection/(°)	5.250–76.612
Max., min. transmission	0.910, 0.640
Reflections collected	13037
Unique reflections	3697
Reflections with I > 2σ(I)	3399
R_{int}	0.0296
R_1[a], wR_2[b] [I > 2σ(I)]	0.0676/0.2021
R_1[a], wR_2[b] [all data]	0.0705/0.2055
Goodness−of−fit on F^2	1.076
Max/min Δρ (e Å^{-3})	2.13/−0.66

[a]$R_1 = \sum||F_0| - |F_c||/\sum|F_0|$, [b]$wR_2 = \{\sum[w(F_0^2-F_c^2)^2]/\sum(F_0^2)^2\}^{1/2}$

Table 2 Selected bond lengths and bond angles for compound **1**

Bond lengths (Å)			
Zn1−O1	2.153(3)	Zn1−N2	2.015(3)
Zn1−O2	2.161(3)	Zn2−N7#1	2.008(3)
Zn1−N9#2	2.041 (3)		
Bond angles (°)			
O1−Zn1−O2	174.62(10)	N2−Zn1−O1	88.46(12)
N2−Zn1−O2	90.02(12)	N2−Zn1−N9#1	122.68(14)
N7#2−Zn1−O1	88.17(12)	N7#2−Zn1−O1	88.84(12)
N7#2−Zn1−N2	129.79(14)	N7#2−Zn1−N9#1	107.52(13)
N9#1−Zn1−O1	92.77(13)	N9#1−Zn1−O2	92.40(13)

Symmetric code: #1 3/2−*x*, *y*, −*z*; #2 1−*x*, *y*, −1/2 + *z*

Zn(II) CPs based on tetrazole-based and pyridyl-based ligands [26, 27]. The $DTPP^{2-}$ ligand adopts a μ_3-coordinate mode in which it binds to three Zn(II) ions with two tetrazole groups and one pyridyl group (Fig. 1). Although

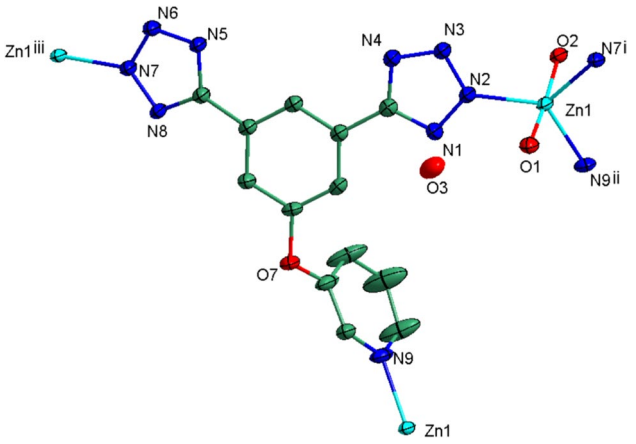

Fig. 1 The coordination environment of Zn(II) and the coordination mode of H_2DTPP drawn at 50% probability ellipsoids. H atoms have been omitted for clarity. Symmetry codes: (i) 1−x, y, −1/2 + z; (ii) 3/2−x, y, −z; (iii) 1−x, y, 1/2 +z

the coordination modes of the two tetrazolyl groups in the $DTPP^{2-}$ ligand are the same, the dihedral angles between the two tetrazole groups and the central benzene ring are different: 11.71(14)° and 7.65(14)°, respectively.

The combination of Zn(II) ions and $DTPP^{2-}$ ligands gives rise to a 2D coordination network extending along the *ac* plane, as shown in Fig. 2. From a topological perspective, both Zn(II) ions and $DTPP^{2-}$ can be seen as three connected nodes; thus, the overall 2D network can be simplified as a $(4{\cdot}8^2)$ topological network. Such topology is usually observed in 2D coordination polymers [28–30].

Furthermore, the adjacent 2D networks are connected by various O–H···N hydrogen bonds between the coordinated H_2O molecule and the uncoordinated N atoms on the tetrazole group (Table 3), resulting in a 3D supramolecular framework, as shown in Fig. 3a and Fig. 3b. Small pores along the *b* direction were observed, as shown in Fig. 3c. It exhibits a percent effective free volume of 10.9% (a total potential solvent volume of 805 Å^3 out of every unit cell volume of 7353 Å^3), as calculated by PLATON software [31].

Phase Purity and Thermal Stability

The phase purity of compound **1** was determined by powder X-ray diffraction (PXRD). As shown in Fig. 4, the position of the diffraction peak obtained from the experimental pattern is basically consistent with that from the simulated pattern, indicating that compound **1** has a high phase purity. The dissimilarity in reflection intensity between them may be attributed to the preferred orientation of the compound **1** sample during data collection.

The thermal stability of compound **1** was measured by thermogravimetric analysis (TGA) from room

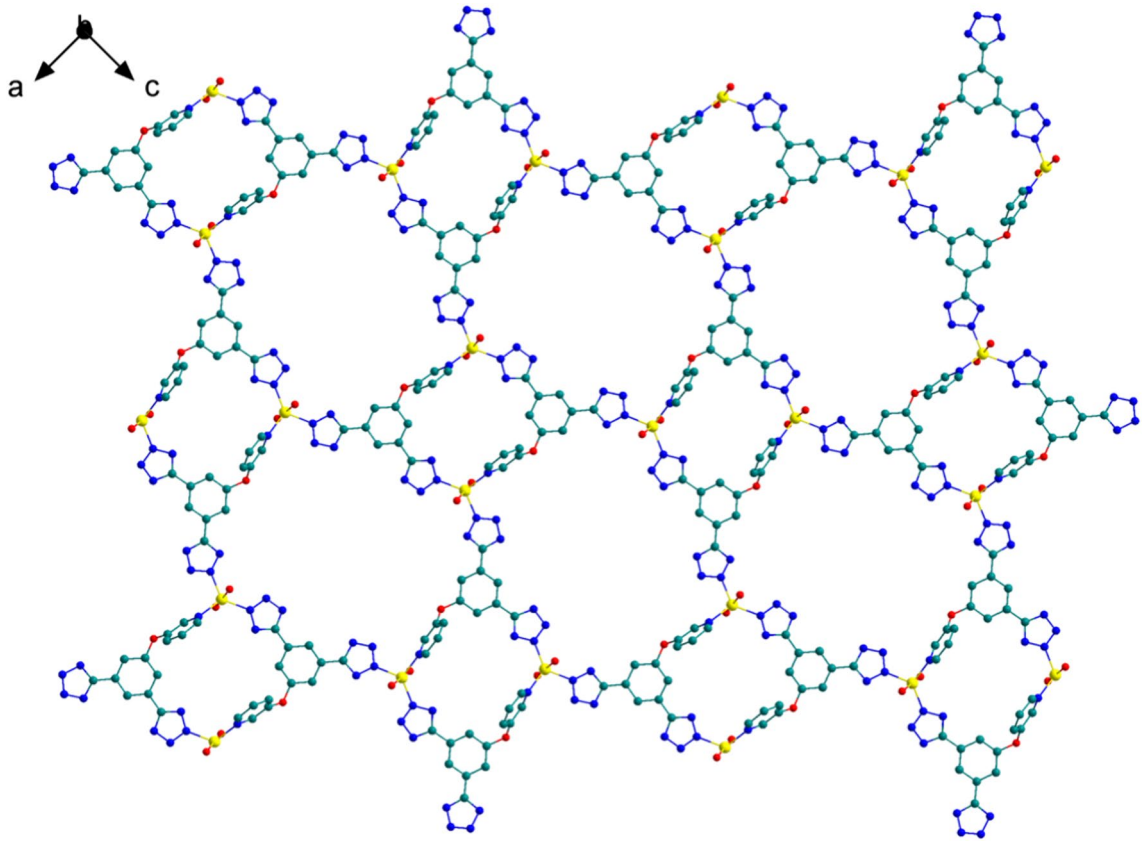

Fig. 2 The 2D network of Compound **1**

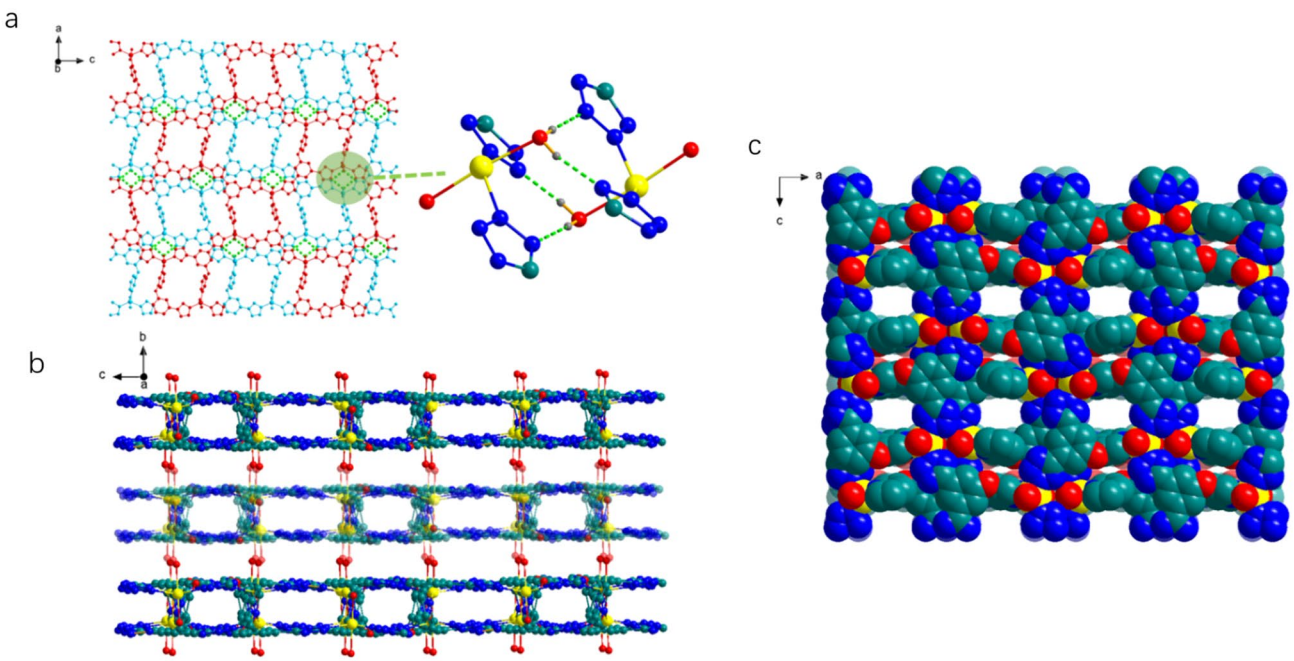

Fig. 3 **a** The hydrogen bonds between two adjacent 2D network in Compound **1**. **b** The 3D supramolecule framework in compound **1**. **c** The small channels in compound **1**

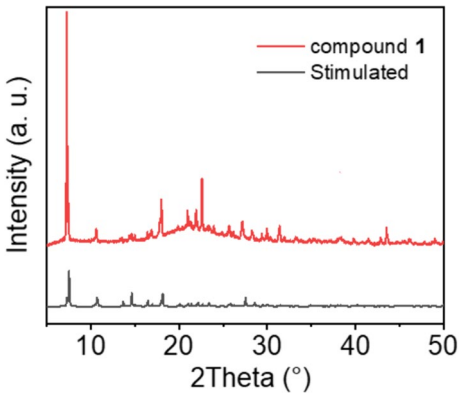

Fig. 4 The experimental and simulated PXRD of compound **1**.

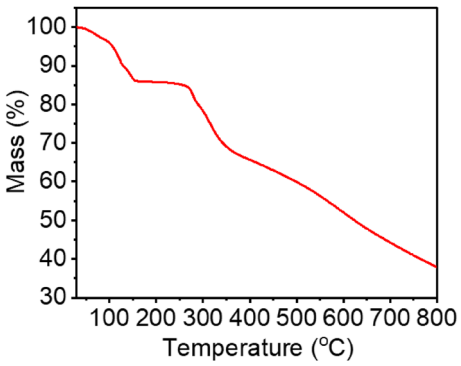

Fig. 5 TGA curve for compound **1**

temperature to 800 °C in a nitrogen atmosphere at a rate of 10 °C min^{-1}. As displayed in Fig. 5, the weight loss of 4.5% from room temperature to 110 °C may be due to the release of uncoordinated water molecules (Calc. 4.2%). The secondary weight loss of 9.0% from 110 to 150 °C may be attributed to the removal of two coordinated water molecules (Calc. of 8.4%). A sharp weight loss is observed above 270 °C, indicating decomposition of the coordination framework.

Fluorescence Properties

Zn(II) CPs generally exhibit photoluminescent properties [32, 33]. Therefore, the photoluminescence of compound **1** was evaluated. As shown in Fig. 6, compound **1** exhibited strong blue luminescence with a maximum emission band at 345 nm when excited at 276 nm in the solid-state at room temperature. For comparison, the photoluminescence of H_2DTPP was also measured. The results showed an emission band centered at 350 nm when excited at 248 nm. Compound **1** only exhibited a slight blueshift of 5 nm compared with that of H_2DTPP. In addition, the shapes of the emission peaks for compound **1** and H_2DTPP are similar. Thus, the emission of compound **1** may be attributed to intraligand transitions.

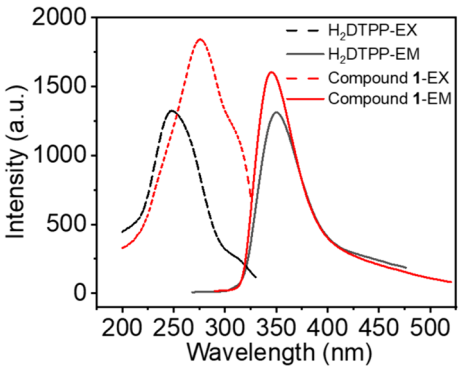

Fig. 6 Excitation and emission of H_2dDTPP and compound **1** in the solid-state at room temperature

Properties of Metal Ion Sensing

The ability of compound **1** to sense metal ions was investigated. The selected metal ions were added to the aqueous suspension of compound **1**, and their photoluminescence spectra were recorded. The results showed that the emission of the compound **1** suspension strongly quenched after the addition of Fe^{3+}, Cu^{2+}, and Ag^{+}, indicating that compound **1** may have the ability to sense these ions and may be most sensitive to Fe^{3+} (Figs. 7a and S1). The sensitivity of the compound **1** suspension for detection in water was further determined. The photoluminescence intensities of the compound

Table 3 Selected details of the hydrogen bonds in compound **1**

	Symmetry code	d(D–H)/Å	d(H···A)/Å	d(D···A)/Å	∠ D–H···A/°
O1–H1A···O3	–	0.87	1.82	2.666(5)	163
O1–H1B···N5	−x + 1, −y + 1, −z	0.87	1.94	2.806(4)	173
O2–H2A···N3	−x + 1, −y + 1/2, z	0.87	1.95	2.814(4)	174
O2–H2B···N8	x, −y + 1/2, z−1/2	0.87	1.99	2.847(4)	168
O3–H3A···N4	−x + 1, −y + 1, −z	0.87	1.98	2.830(5)	165

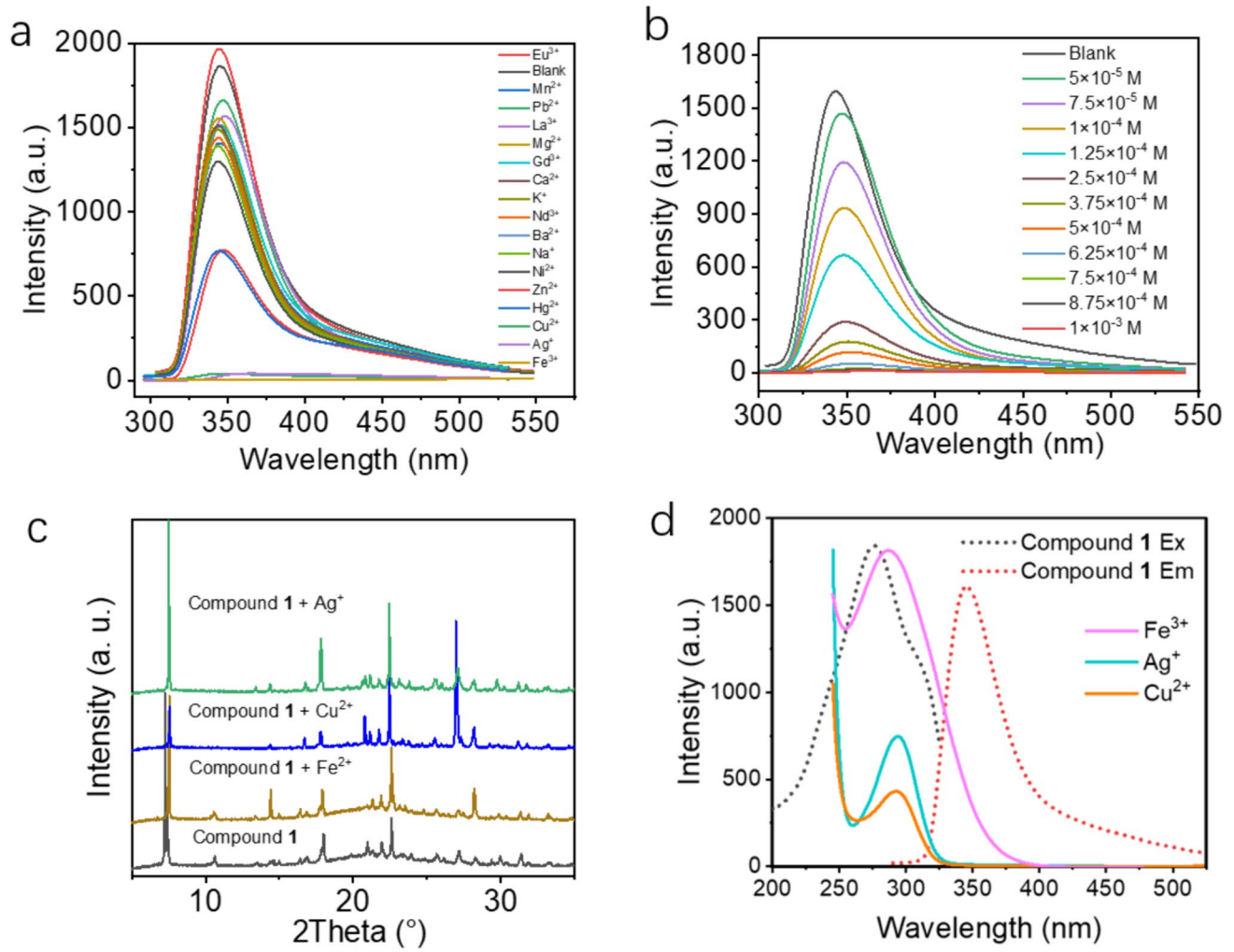

Fig. 7 **a** Luminescence spectra of compound **1** in aqueous solutions containing various cations (0.5 M). **b** Luminescence spectra of compound **1** with various concentrations of Fe^{3+} ions in aqueous solutions. **c** The PXRD of compound **1** before and after immersing in aqueous solutions containing Fe^{3+}, Cu^{2+}, and Ag^{+}. **d** Compare the UV−vis spectra of Fe^{3+}, Cu^{2+}, and Ag^{+} with the excitation and emission spectra of compound 1

1 suspensions with different Fe^{3+}, Cu^{2+}, and Ag^{+} concentrations are shown in Figs. 7b and S2-S4. As shown in Fig. 7b, the luminescence intensity at 345 nm decreased as the concentration of Fe^{3+} increased. The linear relationship between I_0/I and the Fe^{3+} concentration is in the range of 5×10^{-4}–1×10^{-3} M. Consequently, the LOD is calculated to be 1.30×10^{-5} M. These LODs are more moderate than those of some reported MOF sensors [34, 35]. For Cu^{2+} and Ag^{+}, the LODs are 5.64×10^{-2} and 5.06×10^{-2}, respectively, which are higher than those for Fe^{3+}.

The quenching of the fluorescence emission of MOFs by metal ions may be due to structural collapse, energy transfer, competition, etc. [35–39]. The PXRD pattern of compound **1** after immersion in solutions containing 0.1 M Fe^{3+}, Cu^{2+}, and Ag^{+} ions showed that the crystal structures were retained (Fig. 7c); thus, quenching was not caused by structural collapse. In addition, the FT-IR spectra (Fig. S5) of the ion-treated sample remained unchanged, further revealing that compound **1** has a stable crystal structure. To determine whether energy transfer and/or competition occurred. The liquid UV−Vis spectra of Fe^{3+}, Cu^{2+}, and Ag^{+} were measured. The results showed that they have a broad absorption between 250 and 350 nm for Cu^{2+} and Ag^{+} and between 250 and 375 nm for Fe^{3+}. These bands covered the majority of the absorption band of compound 1. Consequently, these metal ions competed to absorb the energy of the light source when excited light passed, resulting in quenching [39]. For the Fe^{3+} ion, there is also some overlap between the absorption spectrum of Fe^{3+} and the emission spectrum of compound 1; therefore, energy transfer from compound **1** to the Fe^{3+} ion also contributed to fluorescence quenching.

Conclusions

In conclusion, we successfully constructed and structurally characterized a new Zn(II) CPs synthesized from a new tripodal N-containing heterotopic ligand. The compound displays a 2D network structure with a ($4{\cdot}8^2$) topology and exhibits blue photoluminescent emission. In addition, it showed the ability to sense Fe^{3+} via photoluminescence quenching. This work indicates that a tripodal N-containing heterotopic ligand with two pyridyl and tetrazolyl groups is an effective organic ligand for the construction of new CPs.

Supplementary Information The online version contains supplementary material available at https://doi.org/10.1007/s10870-024-01023-4.

Acknowledgments The authors gratefully acknowledge the financial support provided by the National Natural Science Foundation of P. R. China (Grant Nos. 22171092, 92056113 and 22073032) and the Science and Technology Project of Qingyuan (2023KJJ013).

Author Contributions Bing-Xun Zhou perform the syntheisis and crystal structure solution of compound 1, and wrote the original draft. Xian Lin, and Hui-Qi Xie perform the characterization of compound 1. Liang-Hua Wu and Chu-Hong Zhang help to prepare figures 1–7. Hai-Yan Song and Sheng-Run Zheng provide the conceptualization, review and editing the manuscript. Jun Fan help to analysis the data.

Data Availability Crystallographic data of the compound **1** (CSD 2339096) was deposited at the Cambridge Crystallographic Data Centre and could be obtained free of charge upon application to CCDC, 12 Union Road, Cambridge CB21EZ, UK [fax: (+44) 1223-336-033; email: deposit@ccdc.cam.ac.uk].

Declarations

Conflict of interest The authors declare no competing interests.

References

1. Furukawa H, Cordova KE, O'Keeffe M, Yaghi OM (2013) Science 341:1230444
2. Chen G, Liu G, Pan Y, Liu G, Gu X, Jin W, Xu N (2023) Chem Soc Rev 52:4586–4602
3. Siu B, Chowdhury AR, Yan Z, Humphrey SM, Hutter T (2023) Coord Chem Rev 485:215119
4. Fan Y, Zheng H, Labalme S, Lin W (2023) J Am Chem Soc 145:4158–4165
5. Iliescu A, Oppenheim JJ, Sun C, Dincă M (2023) Chem Rev 123:6197–6232
6. Li JR, Sculley J, Zhou HC (2012) Chem Rev 112:869–932
7. Zhang JP, Zhang YB, Lin JB, Chen XM (2012) Chem Rev 112:1001
8. Yoshioka S, Inokuma Y, Duplan V, Dubey R, Fujita M (2016) J Am Chem Soc 138:10140
9. Brunet G, Safin DA, Korobkov I, Cognigni A, Murugesu M (2016) Cryst Growth Des 16:4043
10. Schmidt BM, Osuga T, Sawada T, Hoshino M, Fujita M (2016) Angew Chem Int Ed 55:1561
11. Zheng SR, Yang QY, Liu YR, Zhang JY, Tong YX, Zhao CY, Su CY (2008). Chem Commun. https://doi.org/10.1039/B711457E
12. Fu HR, Xu ZX, Zhang (2015) J Chem Mater 27:205
13. Feng Y, Cai SL, Gao Y, Zheng SR (2018) J Solid State Chem 265:64–71
14. Deng SQ, Mo XJ, Zheng SR, Jin X, Gao Y, Cai SL, Fan J, Zhang WG (2019) Inorg Chem 58:2899–2909
15. Deng SQ, Miao YL, Tan YL, Fang HN, Li YT, Mo XJ, Cai SL, Fan J, Zhang WG, Zheng SR (2019) Inorg Chem 58:13979–13987
16. Feng Y, Zou MY, Hu HC, Li WH, Cai SL, Zhang WG, Zheng SR (2022) Chem Commun 58:5013–5016
17. Feng Y, Wu LH, Zhang CH, Zhou BX, Zheng SR, Zhang WG, Cai SL, Fan J (2023) Dalton Trans 52:12087–12097
18. Deng SQ, Mo XJ, Cai SL, Zhang WG, Zheng SR (2019) Inorg Chem 58:14660–14666
19. Wang GQ, Huang JF, Huang XF, Deng SQ, Zheng SR, Cai SL, Fan J, Zhang WG (2021) Inorg Chem Front 8:1083–1092
20. Xian JY, Yang KL, Wang HN, Feng ML, Cai SL, Song HY, Zheng SR, Zhang WG (2021) Inorg Chem Commun 130:108720
21. Xian JY, Huang ZY, Xie XX, Lin CJ, Zhang XJ, Song HY, Zheng SR (2022) Chinese J. Struct Chem 42:100005
22. CrysAlis^{Pro} Software System (2021) Rigaku Oxford Diffraction
23. Dolomanov OV, Bourhis LJ, Gildea RJ, Howard JAK, Puschmann H (2009) J Appl Cryst 42:339–341
24. Sheldrick GM (2015) Acta Crystallogr Sect A Found Adv 71:3–8
25. Sheldrick GM (2015) Acta Crystallogr Sect C Struct Chem 71:3–8
26. Lin H, Liu Y, Ji M, Zhao J, Liu G (2020) Inorg Chem Commun 112:107734
27. Yu H, Sun J (2021) CrystEngComm 23:1744–1755
28. Li K, Blatov VA, Fan T, Zheng TR, Zhang YQ, Li BL, Wu B (2017) CrystEngComm 19:5797–5808
29. Li TT, Liu YM, Wang T, Zheng SR (2017) Inorg Chem Commun 84:5–9
30. Han YH, Zeng DR, Li JM, Wang XL, He KH, Fang ZJ, Shi ZF (2018) J Coord Chem 71:2674–2690
31. Spek AL (2005) PLATON, a multipurpose crystallographic tool. Utrecht University, Utrecht
32. Naresh K, Roopa BV, Kumar M (2021) Coord Chem Rev 427:213550
33. Xie W, Wu J, Hang X, Zhang H, Shen K, Wang Z (2021) Front Chem 9:708314
34. She M, Wang Z, Chen J, Li Q, Liu P, Chen F, Zhang S, Li J (2021) Coord Chem Rev 432:213712
35. Mukherjee D, Pal A, Pal SC, Saha A, Das MC (2022) Inorg Chem 61:16952–16962
36. Han LJ, Yan W, Chen SG, Shi ZZ, Zheng HG (2017) Inorg Chem 56:2936–2940
37. Wang H, Qin J, Huang C, Han Y, Xu W, Hou H (2016) Dalton Trans 45:12710–12716
38. Han LJ, Kong YJ, Hou GZ, Chen HC, Zhang XM, Zheng HG (2020) Inorg Chem 59:7181–7187
39. Liu HF, Tao Y, Wu TX, Li HY, Zhang XQ, Huang FP, Bian HD (2022) Appl Organomet Chem 36:e6456

Authors and Affiliations

Bing-Xun Zhou[1] · Xian Lin[1] · Hui-Qi Xie[1] · Liang-Hua Wu[1] · Chu-Hong Zhang[1] · Hai-Yan Song[1] · Jun Fan[1,2] · Sheng-Run Zheng[1]

✉ Hai-Yan Song
songhaiyan@m.scnu.edu.cn

✉ Sheng-Run Zheng
zhengsr@scnu.edu.cn

[1] DMPA Key Laboratory for Process Control and Quality Evaluation of Chiral Pharmaceuticals, And Guangzhou Key Laboratory of Analytical Chemistry for Biomedicine, School of Chemistry, South China Normal University, Guangzhou 510006, China

[2] Guangdong Longsmall BioChem Technology Co. Ltd, Qingyuan 511500, China